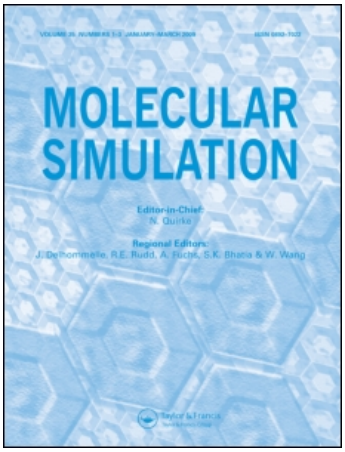

Molecular Simulation
Publication details, including instructions for authors and subscription information:
http://www.informaworld.com/smpp/title~content=t713644482

Self-consistent tight binding model adapted for hydrocarbon systems

D. A. Areshkin[a]; O. A. Shenderova[a]; J. D. Schall[a]; D. W. Brenner[a]
[a] Department of Materials Science and Engineering, North Carolina State University, Raleigh, NC, USA

To cite this Article Areshkin, D. A. , Shenderova, O. A. , Schall, J. D. and Brenner, D. W.(2005) 'Self-consistent tight binding model adapted for hydrocarbon systems', Molecular Simulation, 31: 8, 585 — 595
To link to this Article: DOI: 10.1080/08927020500044988
URL: http://dx.doi.org/10.1080/08927020500044988

Molecular Simulation, Vol. 31, No. 8, July 2005, 585–595

Taylor & Francis
Taylor & Francis Group

Self-consistent tight binding model adapted for hydrocarbon systems

D. A. ARESHKIN*, O. A. SHENDEROVA, J. D. SCHALL and D. W. BRENNER

Department of Materials Science and Engineering, North Carolina State University, Raleigh, NC 27695-7907, USA

(Received July 2003; in final form December 2004)

A self-consistent environment-dependent tight binding method is presented that was developed to simulate eigenvalue spectra, electron densities and Coulomb potential distributions for hydrocarbon systems. The method builds on a non-self-consistent environment-dependent tight binding model for carbon [Tang *et al.*, *Phys. Rev. B* **53**, 979 (1996)] with parameters added to describe hydrocarbon bonds and to account for self-consistent charge transfer. A detailed description of the parameterization procedure is given. Case studies that examine electron emission-related properties of carbon nanotubes demonstrate the utility of the method. The results of these calculations indicate that field enhancement in the vicinity of a nanotube tip is higher for open-ended than for capped nanotubes. At the same time open-ended nanotubes exhibit a higher potential barrier in the tip region. This barrier deteriorates the coupling between conducting states in the nanotube and free electron states in vacuum, and may increase the field emission threshold.

Keywords: Fitting Eigenvalue spectra; Fitting Electron densities; DF-TB

31.15.Ne; 71.15.-m; 79.70. + q; 73.22.-f

1. Introduction

Tight binding (TB) schemes remain the "workhorse" electronic structure method for low-symmetry systems that are too large for fully first principles methods. Indeed, there are now available in the literature numerous TB functional forms and parameterizations for a large number of systems [1]. In the case of carbon, several tight binding models stand out for their ability to describe the electronic and structural properties of a relatively wide range of bonding configurations. Wang, Ho and co-workers, for example, introduced a model in which an electronic energy determined using parameterized on-site and two-center hopping matrix elements is combined with a many-body analytic function to yield reasonable structural and electronic properties of a variety of carbon species [2]. A subsequent model introduced by the same group used two-center hopping matrix elements that depend not only on the distance between the two atoms on which basis functions are centered, but also on the arrangement of neighboring atoms, effectively including three-center integrals in an orthogonal basis [3,4]. This approach, which has been termed an environment-dependent tight-binding (EDTB) model, is the starting point for developing the method described below. In other work, Menon *et al.* introduced a non-orthogonal basis with overlap matrix elements determined from a Huckel-like approach, producing a scheme that also has exceptional transferability for carbon structures [5].

The EDTB model was not the first attempt to include three center integrals in a TB scheme. In 1989, Sankey and Niklewski introduced a parameter free density functional (DF) TB scheme that is essentially a minimal non-orthogonal basis set DF calculation, but with matrix elements precalculated on a coarse grid [6]. Interpolation between grid points is used to evaluate matrix elements for the given set of distances and angles. Frauenheim and co-workers introduced a similar DF-TB scheme based on two-center integrals [7].

The main advantage of the DF-TB schemes over other TB approaches is that in principle they do not require parameter fitting. However, the DF-TB models use a fixed atomic orbital basis, while the EDTB method adjusts hopping integrals to atomic environment. That strategy is analogous to accommodation of the atomic orbitals to atomic environments in DF-like schemes, a potential

*Corresponding author. E-mail: denis@alchemy.nrl.navy.mil

Molecular Simulation
ISSN 0892-7022 print/ISSN 1029-0435 online © 2005 Taylor & Francis Ltd
http://www.tandf.co.uk/journals
DOI: 10.1080/08927020500044988

advantage in terms of the transferability of the scheme for describing electronic states of carbon in different bonding configurations.

To further expand the transferability and functionality of TB schemes, a number of methods have been implemented that introduce self-consistency into TB electronic states (see Ref. [1] for a review). Historically, most of these involved modifications to existing non-self-consistent schemes. For example, Frauenheim *et al.* enhanced a two-center DF-TB approach [7] by adding self-consistent (SC) terms [8,9] and spin polarization [10] that could be used with an $O(N)$ scaling scheme [11]. Similarly, SC versions of Sankey's multicenter DF-TB scheme [12], as well as Halley and coworker's TB approach [13,14] have been introduced, with the latter adding spin-polarized terms to study magnetic systems [15].

In this paper, a SC modification to the EDTB scheme for carbon is introduced that allows charge transfer and applied fields to be modeled. In this approach, which we term the SC-EDTB method, the Hamiltonian matrix H is composed of two parts, the original EDTB matrix $H0$, and SC corrections ΔH. The latter account for charge transfer between constituent atoms, and is supposed to be zero for periodic structures for which the original non-SC EDTB parameterization was made. To be consistent with its initial implementation, the EDTB should be extended to include self-consistency by using a DF based approach analogous to Refs. [8,13,16] but for a basis set that is adjustable to different atomic environments. However, we approach the problem in a less efficient, though simpler manner and use an environment independent basis to compute ΔH.

The atomic basis functions were chosen by fitting to fully first principles molecular spectra and charge distributions. To satisfy an orthogonality requirement imposed by a convergence acceleration scheme that is used in conjunction with the SC-EDTB method [17], and to be consistent with the original EDTB, orthogonality of atomic orbitals is assumed when evaluating the Hartree and exchange integrals required for ΔH. All Hartree integrals are otherwise evaluated exactly. Exchange integrals are evaluated approximately as a first-order expansion over an equilibrium electron density. The correlation potential and hence correlation integrals are neglected. As shown below, the SC-EDTB scheme is highly transferable compared to standard TB, and in many cases produces better results than minimal orthogonal basis set DF or DF TB.

The remainder of this paper is organized as follows. Section II contains a brief description of the original EDTB scheme as introduced by Wang, Ho and co-workers [3,4]. Presented in Section III are the details for computing ΔH, as well as the procedures used to obtain orbital and C—H bond parameters. Section IV contains an application of the SC-EDTB scheme to field emission related properties of single-wall carbon nanotubes. The calculations indicate that that electrons being emitted have to overcome a substantial potential barrier at the tube tip. The height of the barrier for open-ended nanotubes is about two times higher than for capped nanotubes. The final section contains some concluding remarks about the SC-EDTB scheme, including comments regarding the applicability of this method for modeling non-equilibrium electron transport in carbon nanostructures.

2. Environment dependent tight binding scheme

The traditional feature of most TB methods is a two center Hamiltonian matrix parameterization, which implies the neglect of three and four center integrals as well as nonlinearities of the exchange-correlation potential [1]. This means that the contribution of the molecular potential $V(r)$ to the Hamiltonian matrix element $H_{\alpha\beta}$ is restricted to $\langle\varphi_\alpha|V_i(r)|\varphi_\beta\rangle$ where either atomic orbital ϕ_α or ϕ_β belongs to i^{th} atom producing potential $V_i(r)$. To augment the contributions with index i belonging to atomic sites other than those on which ϕ_α or ϕ_β are centered, the original EDTB uses a screening function $S_{\alpha\beta}$ and a scaling function $R_{\alpha\beta}$ that transform the conventional form for two center Hamiltonian matrix elements as $H_{\alpha\beta}(r_{\alpha\beta}) \rightarrow H_{\alpha\beta}[R_{\alpha\beta}(r_{\alpha\beta})](1 - S_{\alpha\beta})$. The parameterized functions $S_{\alpha\beta}$ and $R_{\alpha\beta}$ depend on positions of neighbor atoms, and are designed to account for the influence of atomic environment on two-center Hamiltonian matrix elements. For example, when no other atoms are in the vicinity of the line connecting φ_α or φ_β, $S_{\alpha\beta}$ is zero. When an extra atom appears between φ_α and φ_β the value of $S_{\alpha\beta}$ increases because the contribution to $H_{\alpha\beta}$ comes primarily from the three-center integral.

The function $R_{\alpha\beta}$ has four parameters, and $S_{\alpha\beta}$ uses separate sets of four parameters for each type of hopping integral, allowing a good fit to band structures from DF calculations for six lattice types with atomic coordinations that vary from 2 to 12. The variety of fitted band structures helps to ensure that the EDTB method is applicable to non-periodic systems and is more transferable compared to conventional TB. For example, an indirect bandgap for diamond vs. a direct band gap given by the Xu *et al.* parameterization3 is achieved with the EDTB method.

3. SC-EDTB method

The present section describes modifications made to the EDTB scheme to account for SC charge transfer, and the additional parameterization of matrix elements for C—H bonds. TB may be thought of as a simplified DF scheme for which Hamiltonian elements rather than basis functions are specified. A major simplification of non-SC TB is the assumption of electro-neutrality for each constituent atom. To take charge transfer into account in our SC implementation, a basis set must initially be assumed. After atomic orbitals $\varphi_\zeta(r)$ are chosen, the output electron density $\rho_{\text{out}}(r)$ is evaluated in a standard

manner by using the aufbau principle:

$$\rho_{\text{out}}(r) = \sum_{\substack{\alpha=1,\beta=1 \\ \{\alpha,\beta\}\in \text{Same Atom}}}^{N} \varphi_\alpha(r)\varphi_\beta(r)\sum_{i=1}^{N} f_i Ci_\alpha Ci_\beta f_i$$

$$\equiv f[\varepsilon_i] = \left[1+\exp\left(\frac{\varepsilon_i-\mu}{kT}\right)\right]^{-1}. \quad (1a)$$

Here Ci_ζ is the ζ^{th} component of i^{th} eigenvector of the Hamiltonian matrix $H = H(\rho_{\text{in}}) \equiv H0 + \Delta H(\rho_{\text{in}})$, ρ_{in} is the input electron density from a previous SC iteration, and ε_i is the i^{th} Hamiltonian eigenvalue. Because orbital orthogonality is assumed, Eq. (1a) contains only the products with indexes α and β belonging to the same atom.

Instead of electron densities, uncompensated Mulliken populations (MP)

$$q_{\alpha\beta} = 2\sum_{i=1}^{N/2} Ci_\alpha Ci_\beta - q0_\alpha\delta_{\alpha\beta} \quad \text{if } T=0 \quad (1b)$$

$$q_{\alpha\beta} = 2\sum_{i=1}^{N} f_i Ci_\alpha Ci_\beta - q0_\alpha\delta_{\alpha\beta} \quad \text{if } T>0 \quad (1c)$$

are used below. Here $\delta_{\alpha\beta}$ is the Kronneker delta, and $q0_\alpha$ is the orbital MP in the bulk material for which the EDTB parameterization has been performed. The additional Coulomb potential due to the uncompensated charge is

$$U(r) = \sum_{\substack{\alpha=1,\beta=1 \\ \{\alpha,\beta\}\in \text{Same Atom}}}^{N} q_{\alpha\beta}\int \frac{\varphi_\alpha(R)\varphi_\beta(R)}{|r-R|}dR. \quad (2)$$

$U(r)$ is termed the *additional* Coulomb potential because this electron density is in addition to the reference density from the original EDTB parameterization. If a minimal basis set is used, i.e. four orbitals per carbon and one per hydrogen atom, the reference density for a hydrocarbon system is defined as

$$\rho_{\text{ref}}(r) = \sum_{i\in\text{All Hydrogen Atoms}} \varphi_H(r_i)^2 + \sum_{i\in\text{All Carbon Atoms}} \{q0_s\varphi_s(r_i)^2 + q0_p[\varphi_{px}(r_i)^2+\varphi_{py}(r_i)^2+\varphi_{pz}(r_i)^2]\}. \quad (3)$$

where φ_H, φ_s and $\varphi_{px,py,pz}$ are hydrogen s, and carbon s and p orbitals, respectively, and $r_i = r - R_i$ where R_i is the i^{th} atom position. The original EDTB parametrization was chosen to fit DF band structures for linear, graphite, diamond, simple-cubic (sc), body-centered cubic (bcc), and face-centered cubic (fcc) carbon lattices. In diamond, sc, bcc, and fcc lattices the p-orbital MP's are evenly distributed between the x, y and z p-orbitals. However, the partitioning of the MP's between s and p-orbitals are unique for each lattice type. For example, for the diamond lattice MP's obtained using the original EDTB are $q0_s = 1.20285$ and $q0_p = 0.93238$, while this partitioning is reverted to $q0_s < 1$ and $q0_p > 1$ for the sc lattice. Hamiltonian matrix elements for periodic lattices used in Refs. [3,4] do not need any additional corrections related to local charge transfer. These are accounted for by the EDTB parameters. The additional potential, as given by Eq. (2), should be zero for every periodic lattice used in the EDTB parameterization.

This requirement obviously cannot be satisfied if the basis functions φ_s and $\varphi_{px,py,pz}$ have different radial components, and $q0_s$ and $q0_p$ are assumed to be constants independent of atomic environment. For the sake of simplicity constant $q0_s$ and $q0_p$ values are used that are equal to MP's in diamond. Fortunately, this simplification does not have strong effect on the Hamiltonian. Of the periodic structures used to parameterize the EDTB model for carbon, the linear chain gives the largest magnitude of additional Coulomb potential. Within a small region near the nucleus it achieves a value of ~ 0.7 V, which results in non-physical spectrum line shifts of less than 0.45 eV. Other periodic lattices have smaller deviations from the reference density (3), and hence smaller non-physical additions to the Hamiltonian matrix elements. If a moment decomposition is used for the difference between the electron densities of sp and sp3 hybridized atoms, the lowest-order nonzero moment is a quadrupole. The resulting short-ranged additional Coulomb potential decays as R^{-3}. Therefore it does not have much effect on the overall system spectrum and charge distribution.

After the reference density ρ_{ref} has been chosen it becomes possible to use a first order expansion for the exchange potential $V_{\text{ex}}(\rho) = -\rho^{1/3}(3/\pi)^{1/3}$

$$V_{\text{ex}}[\rho(r)] = V_{\text{ex}}[\rho_{\text{ref}}(r)] + \Delta V_{\text{ex}}$$

where

$$\Delta V_{\text{ex}} \approx \partial_\rho V_{\text{ex}}(\rho)_{\rho=\rho_{\text{ref}}}[\rho(r)-\rho_{\text{ref}}(r)] = \sum_{\substack{\alpha=1,\beta=1 \\ \{\alpha,\beta\}\in \text{Same Atom}}} q_{\alpha\beta}\partial_\rho V_{\text{ex}}(r)_{\rho=\rho_{\text{ref}}}\varphi_\alpha(r)\varphi_\beta(r). \quad (4)$$

Expansion (4) together with Eq. (2) is a key condition for establishing a linear relationship between the input and output MP's that can be utilized, for example, by a Newton-Raphson convergence technique. The overall SC correction $\Delta H_{\alpha\beta}$ to an EDTB matrix element with indices α and β belonging to the same atom is

$$\Delta H_{\alpha\beta} = \sum_{\substack{\gamma=1,\delta=1 \\ \{\gamma,\delta\}\in \text{Same Atom}}}^{N} q_{\gamma\delta}\int\int \frac{\varphi_\alpha(r)\varphi_\beta(r)\varphi_\gamma(R)\varphi_\delta(R)}{|r-R|}dR\,dr + \sum_{\substack{\gamma,\delta \\ \{\alpha,\beta,\gamma,\delta\}\in \text{Same Atom}}} \times q_{\gamma\delta}\int \varphi_\alpha(r)\varphi_\beta(r)\varphi_\gamma(r)\varphi_\delta(r)\partial_\rho V_{\text{ex}}(\rho)_{\rho=\rho_{\text{ref}}}dr. \quad (5)$$

Because of the short range nature of the exchange potential, the summation in the last term is performed only

over indices that belong to the same atom as indices α and β. A common way to approximate $\Delta H_{\alpha\beta}$ when α and β account for the atomic orbitals situated on different atoms is

$$\Delta H_{\alpha\beta} = \frac{1}{2} S_{\alpha\beta}[V(r_\alpha) + V(r_\beta)]. \tag{6}$$

Here V is a sum of applied and additional Coulomb and exchange potentials, r_ζ is the position of the atom on which the ζ^{th} atomic orbital is centered, and $S_{\alpha\beta}$ is the overlap matrix element.

Because an orthogonal basis set is assumed, Eq. (6) is zero. At first, however, it may seem that the quality of a SC-EDTB scheme would benefit if non-zero overlap between neighboring atomic orbitals for Eq. (6) is assumed, while keeping S an identity matrix for eigenproblem solving. The following reasoning is used to show that parameterization benefits in the case where S is a unity matrix. Suppose that the entire system has been placed inside a constant potential field $V(r) = V0$. This shifts the entire eigenvalue spectrum by the amount $V0$, but in all other ways the spectrum should remain unchanged. Indeed, that is the case if $S_{\alpha\beta}$ is the unity matrix, because all diagonal Hamiltonian elements are increased by $V0$, while non-diagonal elements remain intact. The assumption $S_{\alpha\beta} \neq 0$ for $\alpha \neq \beta$ in Eq. (6) leads to the alteration of some of the non-diagonal Hamiltonian elements, and hence to changes other than a mere shift of the whole spectrum. Therefore, the self-consistent correction and the correction due to the applied field are applied only to Hamiltonian elements $H_{\alpha\beta}$ with α and β belonging to the same atom. The correction due to the external electric field with components E_x, E_y and E_z is

$$\Delta H_{\alpha\beta}^{\text{external}} = \int \varphi_\alpha(r)[E_x(x - x_0) + E_y(y - y_0) + E_z(z - z_0)]\varphi_\beta(r)\,\mathrm{d}r. \tag{7}$$

where (x_0, y_0, z_0) is the point where the applied potential equals zero.

A Gaussian basis set is chosen to allow fast analytical evaluation of the Hartree and exchange integrals. The functional forms for carbon and hydrogen atomic orbitals are given by Eqs. (8a) and (8b), respectively,

$$\begin{aligned} \varphi_s &= A_1 \exp(-as_1 r^2) + A_2 \exp(-as_2 r^2) \\ \varphi_{p\alpha} &= 2ap^{5/4}\left(\frac{2}{\pi}\right)^{3/4} X_\alpha \exp(-apr^2) \end{aligned} \tag{8a}$$

$$\varphi_H = a^{3/4}\left(\frac{2}{\pi}\right)^{3/4} \exp(-ar^2) \tag{8b}$$

where X_α is either x, y or z. The coefficient A_2 is obtained from the normalization condition, and A_1, as_1, as_2, and ap are chosen to provide the best fit to DF spectra and charge distributions of cyclic C6 and a C5 linear chain [18(a)]. Because the original EDTB method was developed for pure carbon systems, the parameters $\mathrm{EH_{OnSite}}$, SS_σ, and SP_σ used to describe C—H bond and parameter a for the φ_H atomic orbital must be defined. No interaction between neutrally charged hydrogen atoms is assumed.

In contrast to DFT, TB eigenvalue spectrum is not fixed on the *absolute* scale. The correct positioning of the spectrum on an absolute scale is not necessary if only total energy or forces are desired. Adding the appropriate constant to the TB repulsive term can compensate the constant displacement for each spectrum line. However, the correct absolute position becomes crucial if TB and DF spectra matching is used to define TB orbital or bond parameters. The first step is to obtain the value of constant shift E_{Shift} to be added to every EDTB spectral line to obtain the best fit to a corresponding DF spectra. A brief comment is needed about the quality of TB spectra. The minimal basis set can adequately reproduce low-lying smooth wave functions, and consequently low-lying eigenvalues, but it is insufficient to describe higher energy unoccupied states corresponding to more geometrically involved eigenfunctions. The goal of this parameterization is to obtain electronic properties of the system rather than total energies. For that reason matching both occupied and unoccupied levels is emphasized, at least in the vicinity of Fermi energy. To optimize E_{Shift} the weighed squared differences between the EDTB and DFT spectra for cyclic C6 is minimized. The highest weights were assigned for levels lying near the HOMO and LUMO orbitals, lower weights for other occupied levels, and the lowest weights for high unoccupied levels. The resulting value of E_{Shift} is -5.96 eV. Plotted in figure 1 are DF and EDTB spectra for cyclic C6, where the latter is shifted by E_{Shift}.

The next step is to find A_1, as_1, as_2 and ap coefficients for carbon orbitals. These parameters were obtained by matching C5 linear chain and cyclic C6 MP's and SC-EDTB spectra lines (shifted by E_{Shift}) to their DFT counterparts. However, an issue inherent to many parameterization problems is encountered. The target function (TF) for parameter optimization usually includes several target subfunctions. For example, when optimizing parameters for carbon orbitals it is desirable to minimize the squared deviations for eigenvalues in two different molecules, linear C5 and cyclic C6. Furthermore the TF should include squared MP deviations for cyclic C6, together with squared MP deviations for linear C5 in various applied electric fields. To ensure the correct weights for different target subfunctions accounting for charge and energy, the derivative of onsite SC-EDTB Hamiltonian matrix elements is evaluated with respect to the total MP on that site. Although these derivatives may vary substantially depending on a particular atom in a C5 chain, they still provide an idea of how MP deviations should be weighted if one needs to add them to deviations of

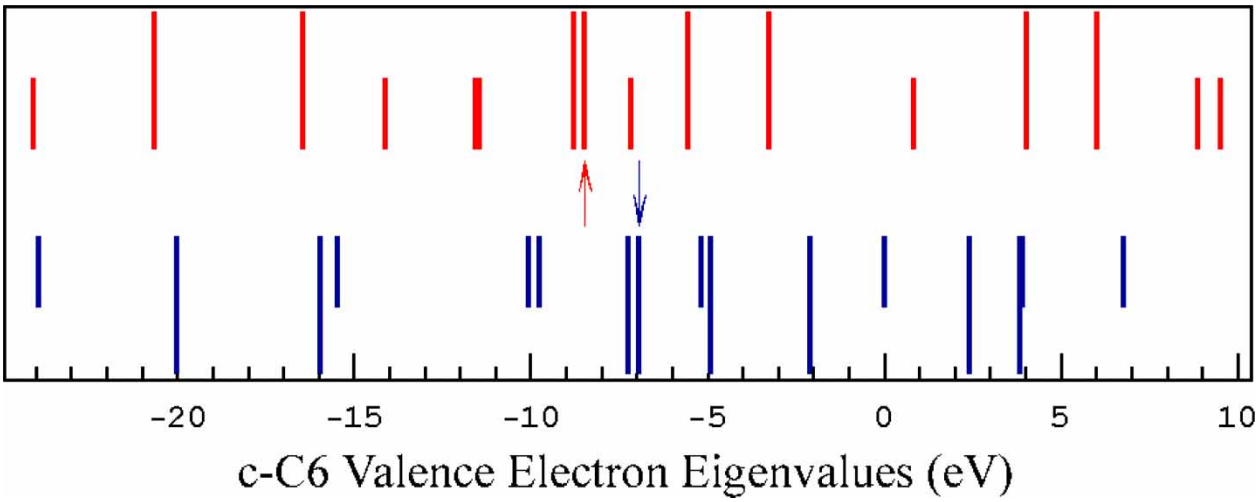

Figure 1. DFT (top) and SC-EDTB (bottom) spectra for cyclic C_6. The line lengths are proportional to the degeneracy of the levels; short lines correspond to non-degenerate levels. The C_6 ring spectrum as well as all other SC-EDTB spectra shown below are shifted by $E_{\text{Shift}} = -5.96\,\text{eV}$.

energy levels:

$$\text{TF} = \sqrt{\sum_i \left[E_i^{\text{DFT}} - \left(E_i^{\text{SCEDTB}} + E_{\text{Shift}}\right)\right]^2} + \left\langle \frac{\partial EOnSite_k^{\text{SCEDTB}}}{\partial \text{MP}_k} \right\rangle_{k\in\{\text{all atom sites}\}} \times \sqrt{\sum_j \left(MP_j^{\text{DFT}} - MP_j^{\text{SCEDTB}}\right)^2}. \quad (9)$$

Here $\langle\rangle$ denotes averaging over all atoms.

Frequently, the line orders in SC-EDTB and DFT spectra are different. Hence SC-EDTB line order number is an unsuitable argument for choosing its DF counterpart. The analysis of wave function symmetry is the only reliable way to link a SC-EDTB line to its DF analog. Symmetry analysis needs to be performed multiple times because spectra are matched iteratively. The symmetry analysis algorithm becomes too intricate even for molecules like linear C5. A reasonable alternative is spectra moments matching; the sum of squared normalized differences between 20 first spectra moments for linear C5 and cyclic C6 is minimized. The TF also includes linear C5 squared atomic MP deviations for various applied fields. The field is directed along the chain and its magnitude has six different values, 0.0, 0.514, 1.028, 1.542, 2.056 and 2.571 V/Å. In addition, separate values of MP for *s* and *p*-orbitals for cyclic C6 are matched. The values for carbon orbital parameters are given in table 1. Tables 2 and 3 demonstrate the quality of the charge fitting. Plotted in figure 2 are the density of states and potential profile for a diamond cluster composed of 161 atoms. In all potential plots below an additional rather than a full Coulomb potential is depicted. This eliminates short-range potential oscillations associated with single atoms and makes the long-range potential component due to interatomic charge transfer clearly visible. An analytical potential [19] is used to relax clusters presented throughout this paper to their minimum energy configuration.

To complete the parameterization, the hydrogen orbital coefficient a Eq. (8b), and C—H bond parameters $\text{EH}_{\text{OnSite}}$, SS_σ, and SP_σ together with their scaling function must be defined. The scaling functions for SS_σ, and SP_σ are taken

Table 1. Optimized carbon orbital parameters. as_1, as_2 and ap are in Å^{-2}.

A_1	A_2	as_1	as_2	ap
0.08215645	0.5980878	0.1129953	1.500468	1.608523

To conserve orbital normalization high precision is given for these parameter; however, only the two first significant digits have physical meaning. The parameter choice is not unique as the target function is not unique.

Table 2. MP's for a C_5 linear chain in external electric fields of different magnitude.

Field [V/Å]	*Method*	*Atom #1*	*Atom #2*	*Atom #3*	*Atom #4*	*Atom #5*
0.000	SC-EDTB	−0.067	0.231	−0.329	0.231	−0.067
	DFT	−0.001	0.095	−0.188	0.095	−0.001
0.514	SC-EDTB	0.030	0.235	−0.327	0.224	−0.162
	DFT	0.122	0.129	−0.196	0.055	−0.111
1.028	SC-EDTB	0.128	0.236	−0.322	0.215	−0.256
	DFT	0.236	0.146	−0.192	0.024	−0.214
1.542	SC-EDTB	0.227	0.234	−0.314	0.202	−0.348
	DFT	0.353	0.156	−0.185	−0.011	−0.312
2.056	SC-EDTB	0.326	0.229	−0.303	0.187	−0.438
	DFT	0.474	0.159	−0.175	−0.052	−0.405
2.571	SC-EDTB	0.426	0.221	−0.288	0.168	−0.526
	DFT	0.597	0.157	−0.162	−0.098	−0.494

The SC-EDTB values were obtained with the parameters given in Table I.

Table 3. Dipole moment and energy decrease for a C_5 linear chain when it is placed in a 2.571 V/Å external electric field.

	SC-EDTB	*DFT*	*Relative error (%)*
Dipole moment	2.51 e × Å	3.60 e × Å	30
Energy decrease	−3.21 eV	−4.56 eV	30

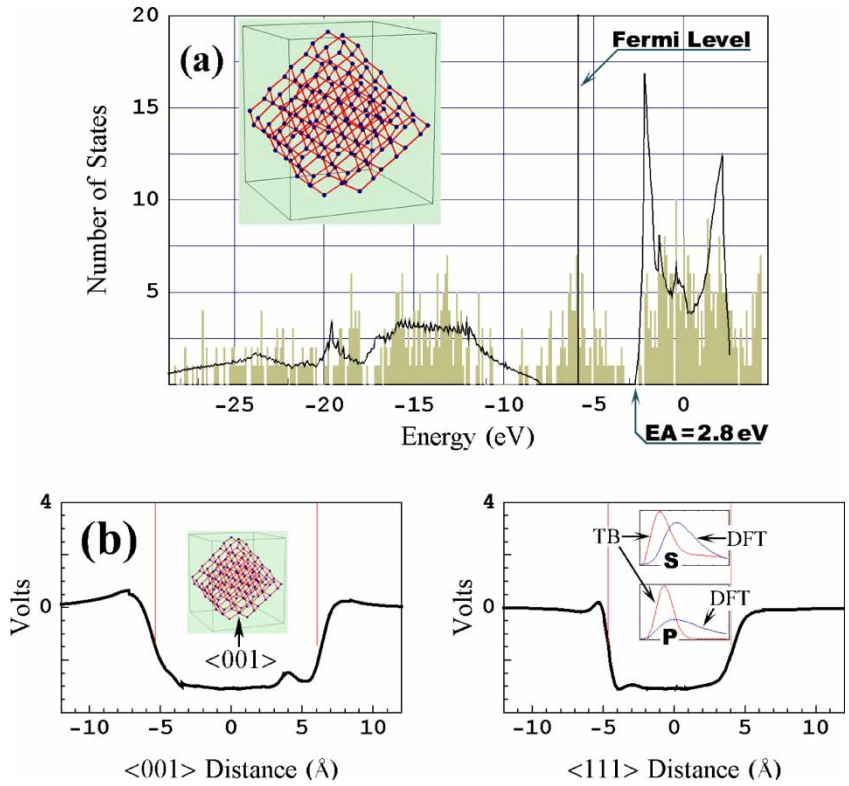

Figure 2. Properties of a diamond cluster (insert) composed of 161 carbon atoms. (a) Spectrum given by the SC-EDTB method. The solid line denotes the SC-EDTB spectrum for bulk diamond. Here and below the bulk spectrum is normalized to give the total number of states equal to the number of carbon valence electrons. In addition to E_{Shift} the bulk spectrum was shifted by -2.9 V, the average Coulomb potential experienced by carbon atoms in the cluster (cf. (b)). (b) The additional Coulomb potential profile along the $\langle 0\,0\,1\rangle$ and $\langle 1\,1\,1\rangle$ lines passing through the center of mass the cluster. The vertical lines mark cluster facets. Right insert shows the radial density distribution (the product of density and squared radius) for *s* and *p*-orbitals.

from the work by Davidson and Pickett [20]. This function reproduces the DF dependence of occupied eigenlevels vs. C—H bond length in methane. At the same time a choice must be made for $\text{EH}_{\text{OnSite}}$, SS_σ, and SP_σ because these parameters complement the SC corrections. In addition, the values for $\text{EH}_{\text{OnSite}}$, SS_σ, and SP_σ given by Davidson and Pickett lead to the wrong signs for MP's for C—H bonds; carbon appears to be less electronegative than hydrogen.

To optimize a, $\text{EH}_{\text{OnSite}}$, SS_σ, and SP_σ, a TF is built that fits MP's and eigenvalue spectra for benzene, methane, and ethane. The TF also includes a subfunction for fitting MP's in a small hydrogen-passivated diamond cluster with $\{1\,1\,1\}$ and $\{1\,0\,0\}$ facets [18(b)]. Spectra moments fitting for benzene and eigenlevel fitting for methane and ethane is performed. Methane levels can be unambiguously identified by their degeneracies; the (un)occupied portion of the methane spectrum has one nondegenerate and one triply degenerate level (cf. figure 3). The ethane 14×14 SC-EDTB Hamiltonian matrix can be broken into $H_{\text{SC NonDIAG}}$, which includes all but the diagonal SC correction elements and non-self-consistent EDTB matrix plus diagonal SC correction elements:

$$H = H_{\text{EDTB+SCDIAG}} + H_{\text{SC NonDIAG}}. \tag{10}$$

Fortunately the secular equation for $H_{\text{EDTB+SCDIAG}}$ can be solved analytically [22]. A particular set of parameters a, $\text{EH}_{\text{OnSite}}$, SS_σ and SP_σ is substituted into the analytical expression for a certain eigenenergy level, its numerical value is obtained, and the SC-EDTB wave function corresponding to this level is identified. Then by analyzing the wave function symmetry it is matched to its DFT counterpart. This determines which numerical DFT level should be matched to the given SC-EDTB analytical eigenenergy expression. The analytical solution establishes links between DFT and SC-EDTB levels by using just *one* particular parameter set, though these links are valid for *any* set of a, $\text{EH}_{\text{OnSite}}$, SS_σ, and SP_σ.

The evaluation of the target subfunction responsible for ethane eigenlevel matching proceeds in the following order. First, an exact numerical SC-EDTB solution for the given parameter set is obtained. Then for each DFT level E_i^{DFT}, its approximate SC-EDTB counterpart E_i^{SCEDTB} (given by the corresponding analytical eigenvalue expression for $H_{\text{EDTB+SCDIAG}}$) is evaluated. The numerical solution gives a SC Hamiltonian matrix, and hence $H_{\text{SCNonDIAG}}$. Treating $H_{\text{SCNonDIAG}}$ as a small perturbation, the first order correction $\delta E_i^{\text{SCEDTB}}$ to E_i^{SCEDTB} is obtained. Then the ethane energy levels target subfunction EthaneTsubF is calculated as

$$\text{EthaneTsubF}(a,\text{EH}_{\text{OnSite}},\text{SS}_\sigma,\text{SP}_\sigma) = \sqrt{\sum_i \text{Weight}_i \left[E_i^{\text{DFT}} - \left(E_i^{\text{SCEDTB}} + \delta E_i^{\text{SCEDTB}} + E_{\text{Shift}}\right)\right]^2}. \tag{11}$$

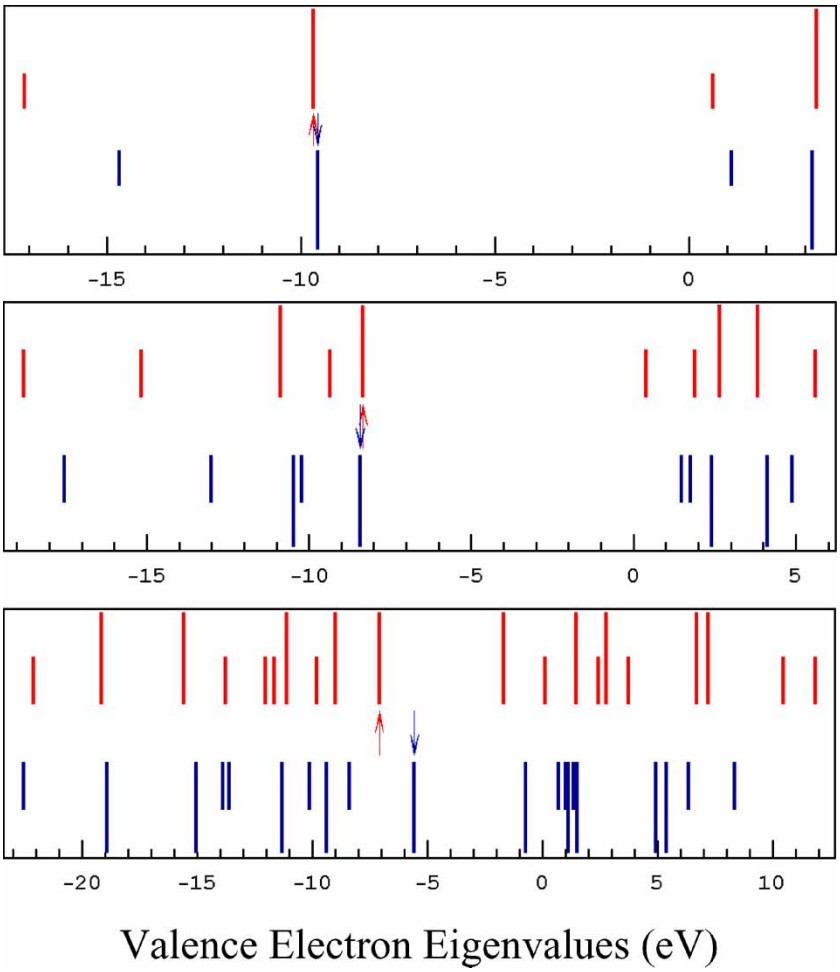

Figure 3. Methane (top), ethane (center), and benzene (bottom) spectra. The upper portion of each plot shows the DFT spectrum, the lower portion shows the SC-EDTB results.

The optimized values of a, EH_{OnSite}, SS_σ, and SP_σ are given in table 4. Table 5 demonstrates the quality of the charge fitting. These values along with those from table I were used to obtain molecular (figure 3) and hydrogen-passivated diamond clusters spectra (figure 4).

The insert in figure 2(b) shows the radial density distribution (the product of density and squared radius) for s and p-orbitals. DF curves were obtained for single carbon atom by using a spin polarized exchange correlation term and large basis set. The s-orbital density is averaged between spin-up and spin-down states. In accord with references [8,16] the orthogonal SC-TB methods use more compact atomic orbitals than DF calculations. The major reason for orbital contraction is the assumption of orthogonality for SC-EDTB orbitals. Non-orthogonal orbital overlap may lead to either an increase or decrease of electron density in the overlap region. However, the extension of the SC-EDTB orbitals always leads to an increase of electron density in the regions where more than one atom contributes to the total charge density, i.e. along interatomic bonds. This leads to a systematic error that lessens the similarity between SC-EDTB and DF calculations.

Table 4. Optimized hydrogen orbital exponential coefficient [$Å^{-2}$], and C—H bond parameters [eV].

a	EH_{OnSite}	SS_σ	SP_σ
2.74101	3.52045	−3.33111	5.49273

If a finite size diamond cluster is considered, the electron affinity (EA) for the crystalline surface prevailing in the cluster (e.g. {1 1 1} in figures 2(a) and 4(a)) can be read directly from the spectral plot. Dimensional effects are not essential for clusters larger than 1 nm. The cluster depicted in figure 2(a) is a metastable system. It is impossible to obtain a clean reconstructed {1 1 1} surface through relaxation of a nano-diamond cluster, because complete energy minimization transforms the cluster into an onion-like fullerene structure [23]. Therefore the EA of 2.7 eV shown in figure 2(a) cannot be compared to the EA measured experimentally [24] or derived from DF simulations [25], which are 0.38 and 0.5 eV, respectively. The large EA value originates from the high electro-negativity of the dangling bonds at the unreconstructed {1 1 1} surface. The reconstructed {1 1 1} surface does not

Table 5. MP's for carbon atoms in hydrocarbon molecules.

	Methane		*Ethane*		*Benzene*	
	SC-EDTB	*DFT*	*SC-EDTB*	*DFT*	*SC-EDTB*	*DFT*
MP *s*-orbital	0.334	0.266	0.240	0.252	0.083	0.167
MP *p*-orbital	0.507	0.815	0.328	0.592	0.121	0.140
MP total	0.840	1.081	0.568	0.844	0.203	0.307

have dangling bonds and we expect the SC-EDTB method to demonstrate a lower EA in that case. The other reason that may account for an erroneously large potential drop at the free diamond surface, and hence for wrong EA values is the orbital shape discrepancies discussed earlier.

At the same time the SC-EDTB model exhibits a much better EA for a hydrogen passivated diamond surface, while DF calculations overestimate the EA by 0.8 eV. Experimental SC-EDTB and DF EA's for a {1 1 1} hydrogenated surface are −1.27, −1.4 and −2.03 eV, respectively. As noted in Ref. [25] only the EA difference ΔEA between clean and passivated surfaces can be calculated reliably, while absolute EA values may contain large errors. Hence, ΔEA is the major quantity that should be used to compare SC-EDTB to DF calculations. The possibly incorrect free surface EA is considered to be the only problematic issue of our parameterization. Note, however, that if a non-SC EDTB is used, the values of the free surface EA based on non-SC MP's will be about 20–30 eV regardless of the orbital shape. All other SC-EDTB tests seem to give a reasonably good fit to DF data.

4. Field enhancement by carbon nanotubes

As a demonstration of the method described in the previous sections we chose a problem related to field emission from carbon nanotubes. The number of carbon atoms in our simulations was between 240 and 300. All simulations were done on a low-end workstation (500 MHz dual Pentium III Xeon).

We start with the question posed in the experimental paper by Bonard and coworkers [26]. Bonard *et al.* found

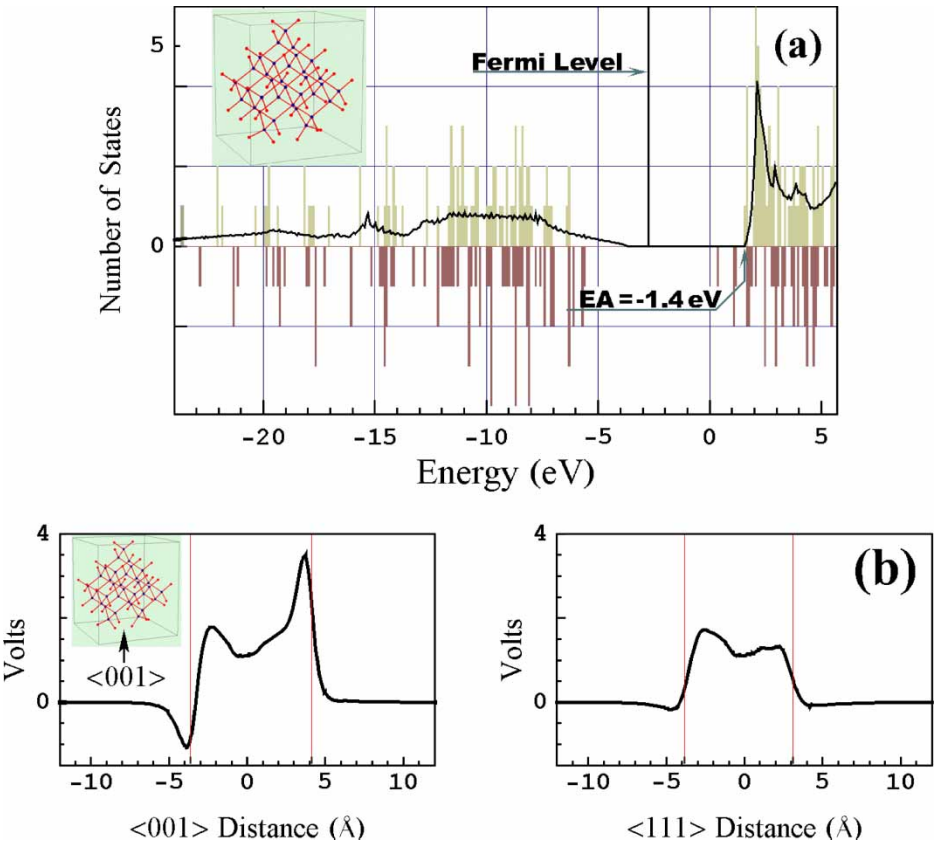

Figure 4. Properties of a hydrogen-passivated diamond cluster (insert) composed of 34 carbon atoms. (a) SC-EDTB (top) and DF (bottom) spectra. In addition to E_{Shift} the bulk spectrum (solid line) was shifted by 1.6 V average Coulomb potential experienced by carbon atoms in the cluster (cf. (b)). Note that the DF result underestimates the bandgap for bulk diamond by approximately 1.0 eV. (b) The additional Coulomb potential profile along ⟨0 0 1⟩ and ⟨1 1 1⟩ lines passing through the center of mass of the cluster. The vertical lines mark cluster facets.

that the emission threshold voltage for metallic capped single wall nanotubes (SWNT) is about two times lower than for open end SWNT. This fact may seem strange since metallic nanotubes behave as perfect conductors (e.g. [21]), and thus the field enhancement is inversely proportional to the tube tip curvature radius. Open-ended nanotubes have sharp edges and therefore are expected to have better field enhancement and lower threshold voltage compared to their capped counterparts.

We performed self-consistent potential calculations for a capped and open-ended 5 × 5 SWNT in a 0.1 V/Å external electric field parallel to the tube axis. The open-ended SWNT is composed of 240 atoms. The capped SWNT has two additional C60 hemispheres which give 300 atoms in total. The length to diameter ratio for the open ended SWNT is 4.3. Figures 5(a,c) show the electron potential along the line lying on the nanotube surface for the open ended and capped SWNT, respectively. Figure 5(b) shows the electron potential through the tube axis for the capped tube. The electric field is directed in such a way that the electron potential increases from left to right as viewed on the figure, and hence electrons are emitted from the left end of the tube. As expected, our simulations show that the field enhancement is larger for open ended SWNT, (see also figure 6). However, it is not the sole factor in determining emission current.

The major difference between potential plots 5(a) and 5(c) is the height of potential barriers at the tube ends. A similar barrier height difference is present when no external field is applied. The local density of states (LDOS) for the tube endcap resembles the LDOS for the infinitely long SWNT, and therefore no strong charge transfer between the SWNT and the endcaps is observed. The edges of the open ended SWNT exhibit a much different LDOS with the Fermi level being lower than those for infinitely long SWNT. The substantial Fermi level difference and strong localization of the edge states result in a large charge pileup at the open ends of the tube. Field emission current is proportional to the coupling between the "bulk" conduction states in SWNT and states in vacuum, which are schematically shown in figure 5. Between these two types of states, there are localized states in the cap of the closed nanotube and at the edges of the open-ended SWNT. The SWNT is metallic in both cases so there is at least one localized state with the energy equal to the Fermi level. We show these states in figure 5 as Gaussian curves. The wave function coupling is proportional to their geometrical overlap. Large charge pile-up at the edge of the open-ended SWNT shows a highly isolated state, which effectively separates conducting states of the tube and vacuum states. Therefore, coupling between the open-ended tube and vacuum occurs primarily in two steps; conducting SWNT states couple to the localized edge states, and the latter couple to states in the vacuum. For the capped SWNT, isolation is not as pronounced and so the coupling is stronger. Coupling may also be

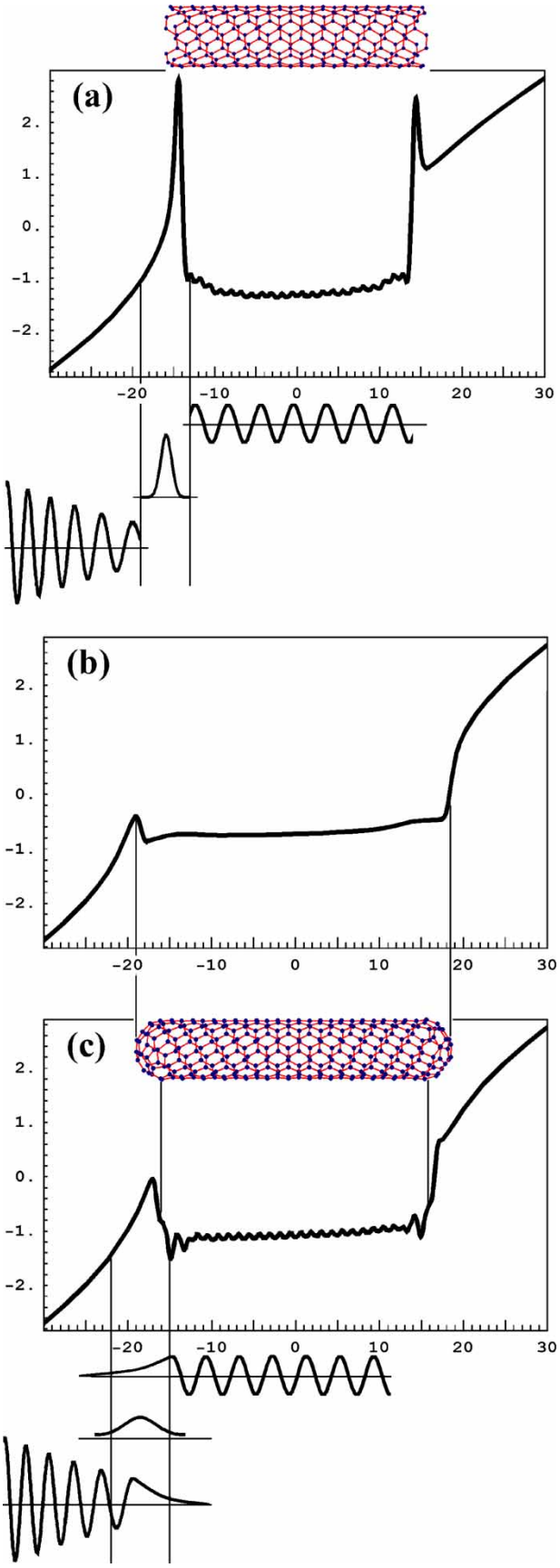

Figure 5. The additional Coulomb potential along the line parallel to a 5 × 5 open-ended (a) and capped (b, c) SWNT. For (a) and (c) the line lies on the SWNT surface; for (b) it coincides with the SWNT axis. Distance is inÅ, potential in eV.

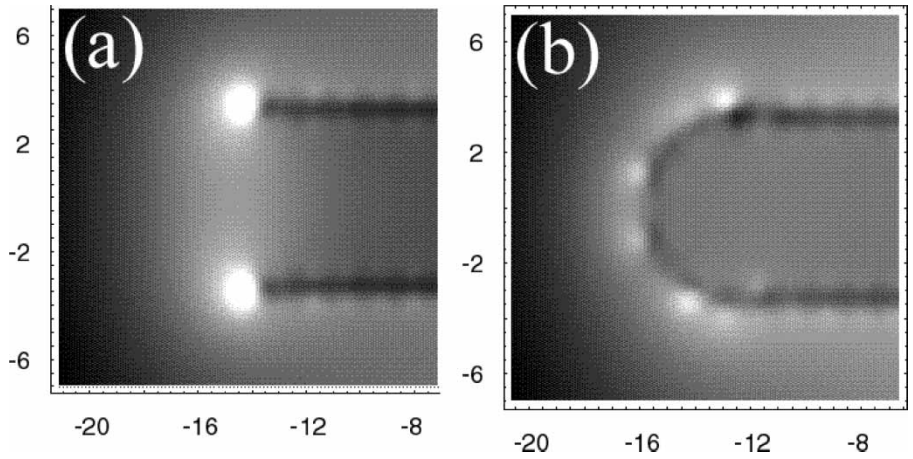

Figure 6. Cross-sectional plots of an additional Coulomb potential for the open-ended (a) and capped (b) SWNTs illustrated in figure 5. The cross-section planes go through the tubes axes. Bright regions correspond to high electron potential.

established directly between tube conducting states and vacuum states.

5. Conclusions

The non-self-consistent EDTB for carbon was extended to a self-consistent scheme for hydrocarbons. The extension was performed in two steps. First, the SC correction was added for carbon only. This correction uses seven parameters, a shift parameter E_{Shift}, reference Mulliken populations $q0_\alpha$, $q0_\beta$, and four orbital parameters for carbon. The second step includes fitting three hydrocarbon bond parameters $\text{EH}_{\text{OnSite}}$, SS_σ, SP_σ, and an orbital exponent a for hydrogen.

Extra parameters required for the self-consistent correction and for C—H bonds were determined by matching MP's and SC-EDTB spectra to their DFT analogs. There may be a discrepancy between the SC-EDTB and DF values of the potential drop at the free diamond surface. All other SC-EDTB results fit DF and experimental data reasonably well. To illustrate SC-EDTB capabilities, field emission properties of single-wall metallic carbon nanotubes were considered. The calculations indicate that field enhancement is stronger for an open-ended nanotube than for its capped variant. At the same time the high potential barrier at the tip of the open-ended nanotube may deteriorate its field emission capability.

Based on several factors, it is anticipated that the SC-EDTB scheme reported here will be extremely useful for transport problems in medium-size (up to 1000 atoms on a PC) carbon nanosystems. To calculate non-equilibrium transport properties, numerical integration of a Green's function matrix is needed, which requires $O(N^3)$ operations for every sampling point on an integration contour. That makes a minimal basis set a substantial computational advantage. Second, the accuracy of the method is comparable to the overall accuracy achieved by means of Green's function techniques. Because most Green's function techniques are not exact, there may be no compelling reason for using an *ab-initio* scheme with a precision that supersedes the overall quality of the method used to evaluate the electron current. Therefore the SC-EDTB method is a reasonable trade-off between fast but non-self-consistent tight binding, and sometimes unnecessarily precise and computationally expensive DF calculations. Finally, orthogonal atomic orbitals are assumed so that a modified Newton–Raphson algorithm for non-linear systems of equations can be efficiently used to achieve self-consistency. As discussed in [17], this new numerical method ensures guaranteed and rapid convergence of SC iterations, even for metallic systems in strong applied fields, and is well suited for both equilibrium and non-equilibrium problems.

Acknowledgements

Helpful discussions with A. Buldum, J-P Lu, J. Mintmire, O. Zhou, and J. Bernholc are gratefully acknowledged. This work was funded by a supplement to the Office of Naval Research Contract N00014-95-1-0279 and through a Multi-University Research Initiative funded by the Office of Naval Research through a subcontract from the University of North Carolina at Chapel Hill.

References

[1] For a review, see. C.M. Goringe, D.R. Bowler, E. Hernandez. Tight-binding modeling of materials. *Rep. Prog. Phys.*, **60**, 1447 (1997).
[2] C.H. Xu, C.Z. Wang, C.T. Chan, K.M. Ho. A transferable tight-binding potential for carbon. *J. Phys.: Condens. Matter*, **4**, 6047 (1992).
[3] M.S. Tang, C.Z. Wang, C.T. Chan, K.M. Ho. Environment-dependent tight-binding potential model. *Phys. Rev. B*, **53**, 979 (1996).
[4] M.S. Tang, C.Z. Wang, C.T. Chan, K.M. Ho. Environment-dependent tight-binding potential model. *Phys. Rev. B*, **54**, 10982 (1996).
[5] M. Menon, K.R. Subbaswamy. Universal parameter tight-binding molecular-dynamics—application to c-60. *Phys. Rev. Lett.*, **67**, 3487 (1991).

[6] O.F. Sankey, D.J. Niklewski. *Ab-initio* multicenter tight-binding model for molecular-dynamics simulations and other applications in covalent systems. *Phys. Rev. B*, **40**, 3979 (1989).
[7] D. Porezag, Th. Frauenheim, Th. Köhler, G. Seifert, R. Kaschner. Construction of tight-binding-like potentials on the basis of density-functional theory—application to carbon. *Phys. Rev. B*, **51**, 12947 (1995).
[8] M. Haugk, J. Elsner, T. Frauenheim, T.E.M. Staab, C.D. Latham, R. Jones, H.S. Leipner, T. Heine, G. Seifert, M. Sternberg. Structures, energetics and electronic properties of complex III–V semiconductor systems. *Phys. Status. Solidi* B **217**, 473 (2000).
[9] M. Elstner, D. Porezag, G. Jungnickel, J. Elsner, M. Haugk, T. Frauenheim, S. Suhai, G. Seifert. Self-consistent-charge density-functional tight-binding method for simulations of complex materials properties. *Phys. Rev. B*, **58**, 7260 (1998).
[10] T. Frauenheim, G. Seifert, M. Elstner, Z. Hajnal, G. Jungnickel, D. Porezag, S. Suhai, R. Scholz. A self-consistent charge density-functional based tight-binding method for predictive materials simulations in physics, chemistry and biology. *Phys. Status Solidi B*, **217**, 41 (2000).
[11] M. Sternberg, G. Galli, T. Frauenheim. NOON—a non-orthogonal localised orbital order-N method. *Comp. Phys. Commun.*, **118**, 200 (1999).
[12] M.-H. Tsai, O.F. Sankey, D. Dow. Charge-transfer in *ab-initio* realspace molecular-dynamics. *Phys. Rev. B*, **46**, 10464 (1992).
[13] J.W. Halley, M.T. Michalewicz, N. Tit. Electronic-structure of multiple vacancies in rutile TiO_2 by the equation-of-motion method. *Phys. Rev. B*, **41**, 10165 (1990).
[14] N. Yu, J.W. Halley. Electronic-structure of point-defects in rutile TiO_2. *Phys. Rev. B*, **51**, 4768 (1995).
[15] M. Zhuang, J.W. Halley. Self-consistent tight-binding method for the prediction of magnetic spin structures in solids: Application to MnF_2 and MnO_2. *Phys. Rev. B*, **64**, 024413 (2001).
[16] K. Esfarjani, Y. Kawazoe. Self-consistent tight-binding formalism for charged systems. *J. Phys.-Condens. Matter*, **10**, 8257 (1998).
[17] D.A. Areshkin, O.A. Shenderova, J.D. Schall, D.W. Brenner. Convergence acceleration scheme for self-consistent orthogonal-basis-set electronic structure methods. *Mol. Simulation*, **29**, 269 (2003).
[18] CERIUS2 4.0 by Molecular Simulations, Inc. was used to compute DFT electronic structure using the following builder: (a) ADF, (b) DMOL3.
[19] D.W. Brenner. Empirical potential for hydrocarbons for use in simulating the chemical vapor-deposition of diamond films. *Phys. Rev. B*, **42**, 9458 (1990).
[20] B.N. Davidson, W.E. Pickett. Tight-binding study of hydrogen on the C(1 1 1), C(1 0 0), and C(1 1 0) diamond surfaces. *Phys. Rev. B*, **49**, 11253 (1994).
[21] L. Lou, P. Nordlander, R.E. Smalley. Fullerene nanotubes in electric fields. *Phys. Rev. B*, **52**, 1429 (1995).
[22] MATHEMATICA 4.0 by Wolfram Research, Inc. was used
[23] J.-Y. Raty, G. Galli, C. Bostedt, T.W. Buuren, L.J. Terminello. Quantum Confinement and Fullerenelike Surface Reconstructions in Nanodiamonds. *Phys. Rev. Lett.*, **90**, 0374701 (2003).
[24] J. Ristein. Electronic properties of diamond surfaces—blessing or curse for devices? *Diam. Relat. Mater*, **9**, 1129 (2000).
[25] M.J. Rutter, J. Robertson. *Ab-initio* calculation of electron affinities of diamond surfaces. *Phys. Rev. B*, **57**, 9241 (1998).
[26] J.M. Bonard, *et al.* Field emission from carbon nanotubes: perspectives for applications and clues to the emission mechanism. *Appl. Phys. A*, **69**, 245 (1999).